ADVANCED MATERIALS
www.advmat.de

High-Brightness Blue Light-Emitting Diodes Enabled by a Directly Grown Graphene Buffer Layer

Zhaolong Chen, Xiang Zhang, Zhipeng Dou, Tongbo Wei, Zhiqiang Liu, Yue Qi, Haina Ci, Yunyu Wang, Yang Li, Hongliang Chang, Jianchang Yan, Shenyuan Yang, Yanfeng Zhang, Junxi Wang, Peng Gao,* Jinmin Li,* and Zhongfan Liu**

Single-crystalline GaN-based light-emitting diodes (LEDs) with high efficiency and long lifetime are the most promising solid-state lighting source compared with conventional incandescent and fluorescent lamps. However, the lattice and thermal mismatch between GaN and sapphire substrate always induces high stress and high density of dislocations and thus degrades the performance of LEDs. Here, the growth of high-quality GaN with low stress and a low density of dislocations on graphene (Gr) buffered sapphire substrate is reported for high-brightness blue LEDs. Gr films are directly grown on sapphire substrate to avoid the tedious transfer process and GaN is grown by metal–organic chemical vapor deposition (MOCVD). The introduced Gr buffer layer greatly releases biaxial stress and reduces the density of dislocations in GaN film and $In_xGa_{1-x}N$/GaN multiple quantum well structures. The as-fabricated LED devices therefore deliver much higher light output power compared to that on a bare sapphire substrate, which even outperforms the mature process derived counterpart. The GaN growth on Gr buffered sapphire only requires one-step growth, which largely shortens the MOCVD growth time. This facile strategy may pave a new way for applications of Gr films and bring several disruptive technologies for epitaxial growth of GaN film and its applications in high-brightness LEDs.

Graphene (Gr) is the first 2D atomic crystal and still gains intense fundamental research and industrial interests owing to its supreme mechanical,[1] electrical,[2] thermal,[3] and optical properties,[4] which provide a wide range of promising applications in field-effect transistors,[5] energy-storage materials,[6] superlubricity,[7] optoelectronics,[8–10] light-emitting diodes (LEDs),[11,12] and many other areas.[13,14] Gr can even provide multiple benefits in some devices/applications, for example, in the applications of LEDs that have been recognized as the third-generation lighting source due to its high-efficiency, environmentally friendly, and long-lifetime properties.[15–17] In specific, the transferred Gr films can serve as transparent conducting electrodes to replace indium tin oxide (ITO) electrodes, especially for deep-UV LEDs on which ITO electrodes are not transparent.[18–20]

Z. L. Chen, Z. P. Dou, Y. Qi, H. N. Ci, Prof. Y. F. Zhang, Prof. P. Gao, Prof. Z. F. Liu
Center for Nanochemistry (CNC)
Beijing Science and Engineering Center for Nanocarbons
College of Chemistry and Molecular Engineering
Peking University
Beijing 100871, China
E-mail: p-gao@pku.edu.cn; zfliu@pku.edu.cn

X. Zhang, Prof. T. B. Wei, Prof. Z. Q. Liu, Y. Y. Wang, Y. Li, H. L. Chang, Dr. J. C. Yan, Prof. J. X. Wang, Prof. J. M. Li
State Key Laboratory of Solid-State Lighting
Institute of Semiconductors
Chinese Academy of Sciences
Beijing 100083, China
E-mail: tbwei@semi.ac.cn; jmli@semi.ac.cn

X. Zhang, Prof. T. B. Wei, Prof. Z. Q. Liu, Y. Y. Wang, Y. Li, H. L. Chang, Dr. J. C. Yan, Prof. J. X. Wang, Prof. J. M. Li
Beijing Engineering Research Center for the 3rd Generation Semiconductor Materials and Application
Beijing 100083, China

The ORCID identification number(s) for the author(s) of this article can be found under https://doi.org/10.1002/adma.201801608.

DOI: 10.1002/adma.201801608

Z. P. Dou, Prof. P. Gao
Electron Microscopy Laboratory
and International Center for Quantum Materials
School of Physics
Peking University
Beijing 100871, China

Z. P. Dou
Key Laboratory for Micro-/Nano-Optoelectronic Devices of Ministry of Education
School of Physics and Electronics
Hunan University
Changsha 410082, China

Prof. S. Y. Yang
State Key Laboratory of Superlattices and Microstructures
Institute of Semiconductors
Chinese Academy of Sciences
Beijing 100083, China

X. Zhang, Prof. S. Y. Yang
School of Microelectronics
University of Chinese Academy of Sciences
Beijing 101408, China

Prof. Y. F. Zhang, Prof. Z. F. Liu
Beijing Graphene Institute (BGI)
Beijing 100095, P. R. China

Prof. P. Gao
Collaborative Innovation Centre of Quantum Matter
Beijing 100871, China

© 2018 WILEY-VCH Verlag GmbH & Co. KGaA, Weinheim

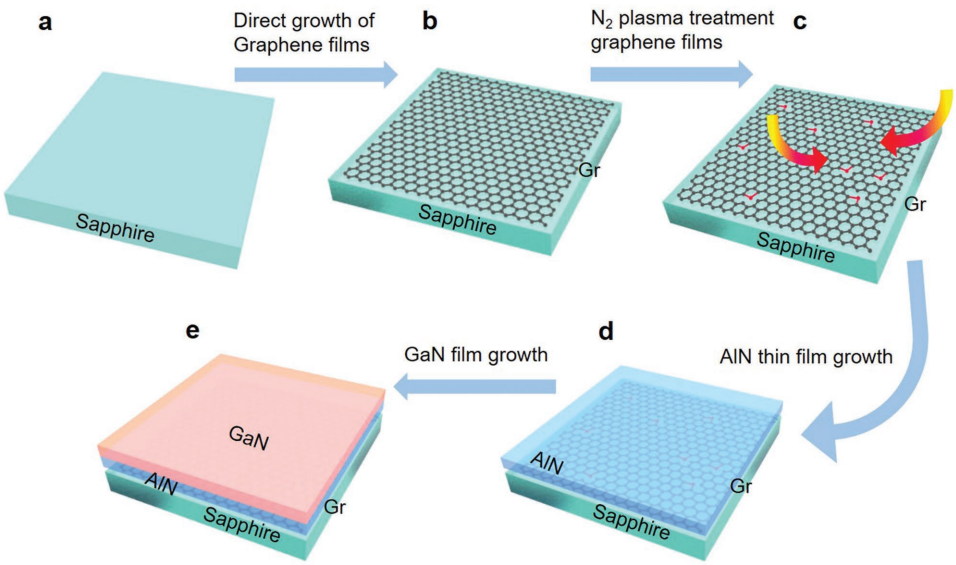

Figure 1. Schematic diagram of the key steps involved in the growth of high-quality GaN films on Gr buffered sapphire substrates. a) Sapphire substrates. b) Direct growth of Gr films on sapphire substrates by using CVD method. c) Gr films are treated in N_2 plasma. d) Growth of high-temperature AlN films on Gr/sapphire substrates by MOCVD. e) Growth of GaN films on AlN/Gr/sapphire.

Gr was also proposed to be a heat dissipation layer to alleviate the self-heating issues when LEDs are operated at high currents.[21] Moreover, Gr could serve as removable layers for epitaxial growth of III-nitride semiconductors (III-Ns), which lights the way for a new field of transferable and flexible LEDs.[11,12,22]

Recently, Gr was also proposed to be as a buffer layer for van der Waals epitaxy growth of GaN film to overcome the substantial thermal expansion coefficient and in-plane lattice constant mismatch between GaN films and sapphire substrates (c-Al_2O_3), which always leads to significant strain in GaN films.[11,23] The biaxial stress in epilayers would generate high density of threading dislocation (TD) and induce piezoelectric polarization in $In_xGa_{1-x}N$/GaN multi-quantum-wells (MQWs), which greatly degrades the performance of LEDs.[24,25] In fact, the growth of low-temperature (LT) GaN buffer layer is a mature process to partially reduce the strain and density of dislocations in GaN film. Compared to the traditional buffer layers, the Gr buffer layer may have some potential advantages, e.g., completely eliminating mismatch, reducing the strain, potential heat dissipation, and transferable nature. However, from previous studies, after introducing the Gr buffer layer, the quality of grown GaN films was found to be significantly degraded, because the low diffusion energy barrier on the Gr surface leads to cluster growth mode, limiting the growth of large-area single-crystalline GaN films.[11] Therefore, the quality of GaN films grown on Gr and light output power (LOP) of transferable LEDs are still far away from the conventional process.[11]

Here, we successfully use Gr films as buffer layer for the growth of high-quality (low stress and low dislocation density) GaN films to improve the performance of LEDs. Gr films are directly grown on c-sapphire substrates to avoid the tedious and cost-ineffective transfer process, which always introduces corrugation, breakage, and defects into the Gr films and would limit the practical application. The Gr is treated in N_2 plasma to create numerous nucleation centers for growth of nitrides. By introducing the Gr layer, the biaxial stress in GaN film is effectively released, leading to the reduced density of dislocations of GaN film and subsequent high quality of MQWs. The as-fabricated high-power LEDs show about 19.1% enhancement in the light output power at injection currents of 350 mA compared with the conventional process derived counterpart. Our work demonstrates a practical application for directly grown Gr films that may bring several disruptive technologies for epitaxial growth of III-Ns and its applications in high-brightness LEDs.

The key processes involved in the growth of high-quality GaN films on the directly grown Gr layers are schematically shown in **Figure 1**. In brief, we directly grow Gr films on sapphire substrates with high scalability by a catalyst-free atmospheric-pressure chemical vapor deposition (APCVD) approach to avoid the complicated and skill-demanding transfer process. Since previous study suggested that large-area single-crystalline GaN thin film could not be grown on pristine Gr films presumably because of the lack of dangling bonds of Gr for nucleation,[11] nitrogen-plasma treatment is applied in our work to introduce defects into Gr film for enhancing its chemical reactivity.[26–29] Although the nitrogen-plasma treatment could increase the GaN nucleation density, the directly grown GaN film always shows clusters with rough and irregular morphology due to the low adsorption energy of Ga atoms on Gr (see Figure S1a, Supporting Information), which is similar with that grown on bare sapphire substrates (see Figure S1b, Supporting Information). Thus, we firstly grow aluminum nitride (AlN) at high temperature on nitrogen-plasma-treated Gr film before GaN growth as the adsorption energy of Al atom on Gr is higher compared to Ga atom.[30]

The typical photograph of as-grown 2 in. Gr/sapphire substrate by the catalyst-free APCVD method shows a nearly same color contrast over the 2 in. wafer, indicating its good uniformity (see Figure S2a, Supporting Information). Scanning electron

© 2018 WILEY-VCH Verlag GmbH & Co. KGaA, Weinheim

15214095, 2018, 30, Downloaded from https://onlinelibrary.wiley.com/doi/10.1002/adma.201801608 by Peking University Health, Wiley Online Library on [03/09/2023]. See the Terms and Conditions (https://onlinelibrary.wiley.com/terms-and-conditions) on Wiley Online Library for rules of use; OA articles are governed by the applicable Creative Commons License

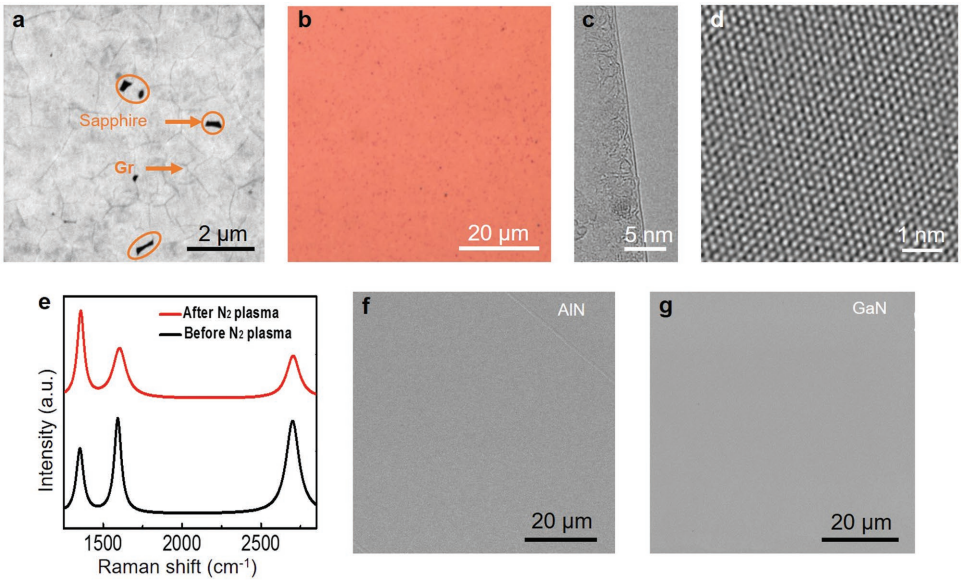

Figure 2. Characterizations of Gr, AlN, and GaN films. a) Scanning electron microscopy (SEM) image of the as-grown Gr films on sapphire substrates. b) Optical microscope image of the as-grown Gr films after transferred onto SiO_2/Si substrate. c) High-resolution transmission electron microscopy (HRTEM) image from the edge of the Gr film showing its monolayer feature. d) Representative HRTEM image of Gr lattice. e) Raman spectra of the as-grown Gr films before (black) and after plasma N_2 treatment (red). f) SEM image of the as-grown flat high-temperature AlN films on sapphire with Gr interlayer. g) SEM image of the as-grown mirror-smooth GaN films on AlN/Gr/sapphire.

microscopy (SEM) image indicates continuous and uniform Gr films could fully cover the substrate (**Figure 2**a). Raman spectra measured from representative positions present similar intensity of D, G, and 2D mode peaks, which confirm the good film uniformity over the lateral distance of 2 in. (see Figure S2b, Supporting Information). The uniformity of the directly grown Gr film is further evaluated by optical microscope inspection after transferred onto the SiO_2/Si substrates, which exhibits the same color contrast at a microscale (Figure 2b). High-resolution transmission electron microscopy (HRTEM) of edge of the Gr film shows its monolayer feature (Figure 2c), which ensures the single-crystalline film growth according to the reported "graphene wetting transparency."[31] In particular, the atomic-resolution HRTEM image shows the high quality of directly grown Gr on sapphire substrates (Figure 2d). In order to increase the chemical activity of Gr for nucleation of nitrides, the Gr film is then exposed to N_2 plasma with 100 Pa and 100 W for 30 s. The Raman spectra in Figure 2e show a significant increase of D peak in the plasma treated Gr compared with the pristine one (Figure 2e). This is attributed to the increase of dangling bonds that are generated during the plasma treatment. Subsequently high-temperature AlN thin film is directly grown on this plasma treated Gr/sapphire substrate via metal-organic chemical vapor deposition (MOCVD). Figure 2f shows an SEM image of a smooth and continuous AlN film grown on plasma-treated Gr/sapphire substrates. In contrast, the morphology of directly grown AlN on sapphire substrates without Gr is rough and discrete as shown in Figure S3a (Supporting Information). X-ray diffraction (XRD) measurement of AlN film grown on a plasma treated Gr/sapphire substrate shows the characteristic peaks at 36° and 76°, which correspond to the (0002) and (0004) planes of wurtzite AlN (see Figure S3b, Supporting Information), respectively. The full width at half maximum (FWHM) of (0002)-AlN X-ray rocking curves with plasma treated Gr interlayers (red line in Figure S3c, Supporting Information, ≈298.8 arcs) is much lower than that without Gr (black line in Figure S3c, Supporting Information, ≈757.3 arcs), which confirms the Gr buffer layer significantly improves the quality of epitaxial AlN films. Thereafter, high-quality, mirror-smooth GaN films are grown on thus-obtained AlN films as illustrated in Figure 2g. It should be noted that there is no need to grow low-temperature buffer layer prior to high-temperature growth of GaN, which is totally different from the traditional process. Another advantage of this method is that direct growth of Gr on the sapphire process can be easily scaled up and cost effective.

The quality of the as-grown GaN films is investigated by atomic force microscopy (AFM), XRD, electron backscatter diffraction (EBSD), and cathodoluminescence (CL) spectroscopy. The as-grown GaN films on plasma treated Gr/sapphire substrates show an atomic terrace surface with the root mean square roughness around 0.67 nm over an area of 10×10 μm^2, as seen in the AFM image in **Figure 3**a. Such smooth surface enables the use of EBSD mapping to identify the crystalline orientations of the GaN epilayer. We find that the as-grown GaN epilayer only exhibits (0001) orientation as indicated in red by the inverse pole figure color triangle (Figure 3b). XRD 2θ profile exhibits intense GaN (0002) and (0004) diffraction peaks at 34.56° and 72.84°, respectively, and weak AlN (0002), (0004) diffraction peaks (see Figure S4, Supporting Information), indicating the (0001) orientation of GaN wurtzite structure. The optical properties of as-grown GaN films are explored by CL with an electron beam acceleration energy of 10 kV. The GaN film exhibits a room-temperature CL peak position at 353 nm with an FWHM of 8.4 nm, indicating a high optical quality of GaN film (see Figure S5, Supporting Information). There is no any bulge in the range of 500–700 nm, further confirming

© 2018 WILEY-VCH Verlag GmbH & Co. KGaA, Weinheim

15214095, 2018, 30, Downloaded from https://onlinelibrary.wiley.com/doi/10.1002/adma.201801608 by Peking University Health, Wiley Online Library on [03/09/2023]. See the Terms and Conditions (https://onlinelibrary.wiley.com/terms-and-conditions) on Wiley Online Library for rules of use; OA articles are governed by the applicable Creative Commons License

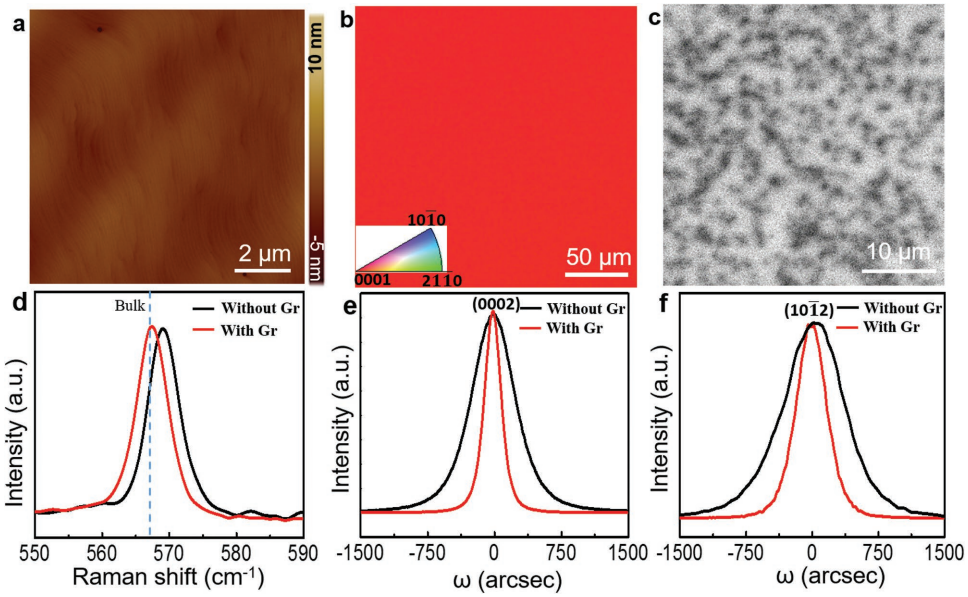

Figure 3. Characterizations of as-grown GaN films on AlN/Gr/sapphire. a) Atomic force microscopy height image of as-grown GaN films with root mean square roughness around 0.67 nm. b) Electron backscatter diffraction mapping of as-grown GaN films showing (0001) single crystallinity. c) Cathodoluminescence mapping of as-grown GaN films featured with low dislocation density. d) Raman spectra of GaN layers grown on sapphire with (red line) Gr interlayers showing redshift compared to that without (black line) Gr interlayers. e) X-ray rocking curves of (0002) and f) (10$\bar{1}$2) GaN films grown on sapphire with (red line) Gr interlayers showing much smaller full width at half maximum (FWHM) compared to that without (black line) Gr interlayers. All the growth parameters of MOCVD were kept identical for Gr buffered and bare sapphire substrates (1045 °C, 6000 sccm NH_3, 80 sccm TMGa, 55 min).

the high-quality nature of as-grown GaN films. Moreover, the CL mapping also allows us to evaluate the density of dislocations in semiconductors. The dark spots in the CL image are ascribed to TD in GaN, which serve as nonradiative recombination centers.[32] Therefore, the TD density of the GaN epilayer is estimated to be ≈1.7×10^7 cm^{-2} in average over a large surface area of 40×40 μm^2, as shown in Figure 3c. The TD density of as-grown GaN on Gr/sapphire is comparable to or even lower than that in the conventional process derived GaN films.[21,33,34]

The stress and dislocation density of as-grown GaN films are further evaluated by Raman spectroscopy and X-ray rocking curve. The Raman spectra of E_2 phonon mode are very sensitive to the biaxial strain in GaN layer.[24,25,35] The stress in GaN therefore can be precisely measured based on the Raman shift. Figure 3d shows the GaN epilayer grown on sapphire substrate undergoes compressive strain, showing a larger frequency (569.2 cm^{-1}) compared with stress-free bulk GaN (567.0 cm^{-1}).[36] In contrast, the corresponding peak position of GaN grown on Gr/sapphire substrate (567.4 cm^{-1}) is almost the same as stress-free bulk GaN (567.0 cm^{-1}). The stress relaxation of GaN epilayer induced by Gr interlayer can be estimated according to $\Delta\omega = K\sigma_{xx}$, where $\Delta\omega$ is the difference of E_2 peak with stress-free GaN crystal value of 567.0 cm^{-1} and K is the stress coefficient ≈2.56 cm^{-1} GPa^{-1}.[24] The biaxial stress values of GaN grown on sapphire and Gr/sapphire substrate are estimated to be 0.86 and 0.16 GPa, respectively, suggesting the effective stain relaxation in GaN layer by the introduction of Gr. The effect of Gr on the quality of GaN layer is further studied by X-ray ω-scan (rocking curve) in Figure 3e,f. The FWHM of the (0002) and (10$\bar{1}$2) rocking curve of GaN is directly related to the density of edge dislocation and screw dislocation in epilayer.[37,38] The (0002) FWHM of GaN epilayer is greatly reduced from 561 to 217 arcs with the assistance of Gr interlayer, and its (10$\bar{1}$2) FWHM is also reduced from 784 to 386 arcs. The estimated densities of screw and edge dislocations of as-grown GaN without Gr are 6.33×10^8 and 1.07×10^{10} cm^{-2}, respectively, while they are reduced to 9.46×10^7 and 5.07×10^9 cm^{-2} with a Gr buffer layer. These results indicate that the Gr film could greatly relax the compressive stress and reduce the dislocation density for improving the quality of GaN epilayer.

Such high-quality GaN films obtained on Gr/sapphire substrates without LT buffer layer enables LED fabrication. Schematic illustration of the fabrication of GaN blue-LED structure is shown in **Figure 4**a. To fabricate LED structures, a 150 nm thick layer of Si-doped n-GaN, 11-period $In_xGa_{1-x}N$/GaN MQWs, and a 150 nm thick layer of Mg-doped p-GaN are deposited on the high-quality, low-stress GaN film grown on Gr/sapphire substrate. Figure 4b and Figure S6 (Supporting Information) show the low magnification cross-sectional scanning transmission electron microscopy (STEM) and energy dispersive spectroscopy (EDS) mapping images of LED heterojunction structure on a Gr/sapphire substrate. The X-ray ω-scan in Figure 4c shows intense satellite peaks in the $In_xGa_{1-x}N$/GaN LED heterostructure on Gr/sapphire substrates, indicating the high quality of MQWs (Figure 4c). In comparison, no such satellite peaks are observed in the $In_xGa_{1-x}N$/GaN heterostructures on bare sapphire substrates without Gr (see Figure S7, Supporting Information). The dark-field image by using the reflection g = 0002 in Figure 4d indicates no dislocations presented in the MQWs, at least not in the inspected area.[39] The high-angle annular dark-field STEM image in Figure 4e shows 11 pairs of MQWs with bright ($In_xGa_{1-x}N$) and dark

© 2018 WILEY-VCH Verlag GmbH & Co. KGaA, Weinheim

15214095, 2018, 30, Downloaded from https://onlinelibrary.wiley.com/doi/10.1002/adma.201801608 by Peking University Health, Wiley Online Library on [03/09/2023]. See the Terms and Conditions (https://onlinelibrary.wiley.com/terms-and-conditions) on Wiley Online Library for rules of use; OA articles are governed by the applicable Creative Commons License

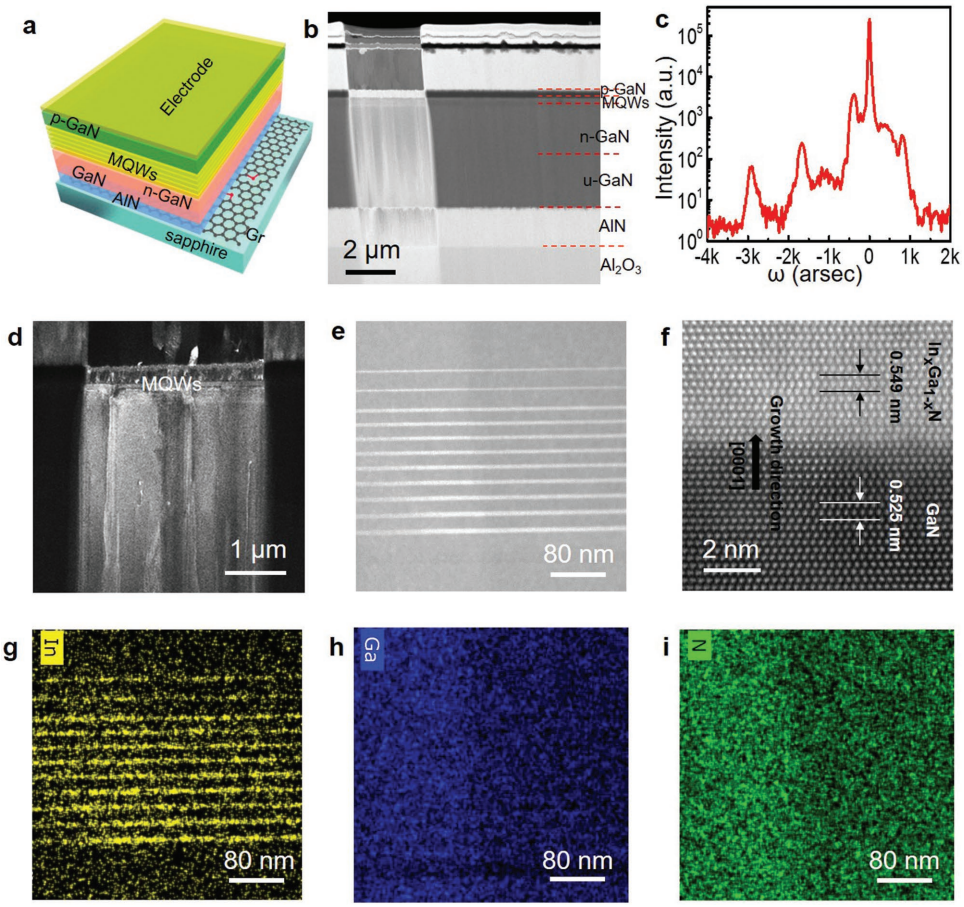

Figure 4. The structure and characterizations of LEDs grown on Gr/sapphire substrates. a) Schematic illustration of the as-fabricated blue LED structure. b) Cross-sectional STEM image of heterojunction LEDs. c) X-ray ω-scan of $In_xGa_{1-x}N$/GaN LED heterostructures with Gr. d) Dark field image of heterostructure with $g = 0002$. e) Cross-sectional STEM image of $In_xGa_{1-x}N$/GaN MQWs in the as-fabricated blue LED. f) Atomic-resolution STEM image of $In_xGa_{1-x}N$/GaN QW lattice. g–i) Corresponding EDS mapping images of In, Ga, and N elements.

(GaN) contrast. The thickness of the $In_xGa_{1-x}N$/GaN MQWs is almost uniform. The selective area electron diffraction pattern of MQWs can be indexed to wurtzite structure (see Figure S8, Supporting Information). The atomically resolved STEM images show abrupt interface and defect free in the $In_xGa_{1-x}N$/GaN MQWs in Figure 4f, and the elemental mapping confirms high quality of quantum wells with uniform distributions of In, Ga, and N elemental in each layer (Figure 4g–i). The interplanar spacing of GaN and $In_xGa_{1-x}N$ was measured to be ≈0.525 and ≈0.549 nm, respectively, corresponding to the d-spacing of GaN (0001) planes.[40,41]

After the electrodes deposition, the LED wafer is diced into 1 mm × 1 mm chips for chip-on-wafer (COW) mapping tests. We also grow the same LED structure on sapphire substrates using the conventional LT GaN buffer layer for comparison. Figure S9a–c (Supporting Information) shows the COW mapping test for LOP value of LED chips with Gr, LED chips without Gr, and conventional process derived LED chips at 350 mA injection current. The corresponding results are sorted out for more clear comparison (Table S1, Supporting Information). The as-fabricated LED chips with Gr show the LOP value is as high as 118.70 mW (Figure S9b, Supporting Information), while only a few can be lighted for the chips without Gr due to the poor crystal quality of GaN (Figure S9a, Supporting Information). In comparison, the LED chips with the conventional process show the LOP values are in the range of 60–100 mW with highest value of 98.78 mW (Figure S9c, Supporting Information), which is lower than that from Gr buffered LED chips (see Table S1, Supporting Information). The small slice size of LED with Gr (15 × 15 mm) leads to the relatively high ratio of chips without light comparing with conventional one (2 in./4 wafer). The COW test results reveal that the Gr buffer layer significantly increases the LOP value of LED chips.

The electroluminescence (EL) performance of the high-power LEDs with and without Gr is further investigated. A typical picture of as-fabricated LED is shown in Figure S10 (Supporting Information). **Figure 5**a shows the current–voltage (I–V) curves of LEDs with and without Gr interlayers, and a conventional LED. The as-fabricated LEDs with Gr show a good rectifying behavior with a turn-on voltage of ≈2.5 V and a low leakage current of 2 mA at −4 V (red line), which is as good as the performance of the conventional LED (blue line). However, the as-fabricated LED without Gr shows a high leakage current even under low input voltages (black line). The LOP of LEDs as a function of injection current is plotted in Figure 5b. The LOP of LEDs increases simultaneously with increasing

 © 2018 WILEY-VCH Verlag GmbH & Co. KGaA, Weinheim

15214095, 2018, 30, Downloaded from https://onlinelibrary.wiley.com/doi/10.1002/adma.201801608 by Peking University Health, Wiley Online Library on [03/09/2023]. See the Terms and Conditions (https://onlinelibrary.wiley.com/terms-and-conditions) on Wiley Online Library for rules of use; OA articles are governed by the applicable Creative Commons License

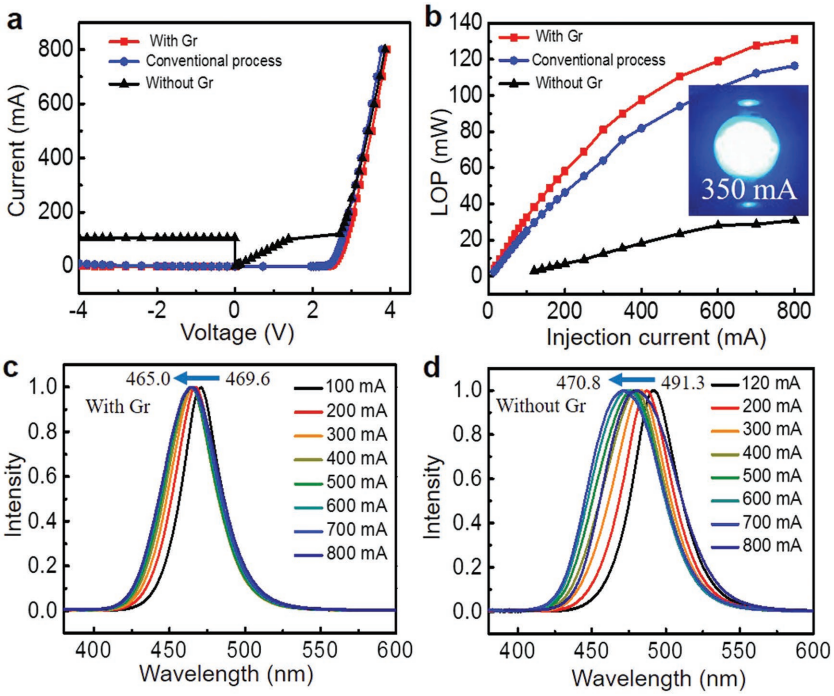

Figure 5. Electroluminescence of LEDs at room temperature. a) Current–voltage characteristics of the as-fabricated LEDs with and without Gr interlayer, and conventional process derived one. b) Light-out power of the as-fabricated LEDs with and without Gr interlayer, and conventional process derived one as a function of injection current. c,d) The normalized electroluminescence spectra as-fabricated LEDs with currents ranging from 100 to 800 mA with Gr (c) and without Gr (d).

the injection current, suggesting that the EL emission generates from the carrier injection and radiative recombination at MQW layers in the LED chips. The LOP of the LED with Gr is much higher than that without Gr due to the improved crystal quality, which is consistent with COW results. It should be noted that the LED with Gr even shows an enhancement of LOP over that of conventional LED with LT GaN buffer, for example, 19.1% enhancement in the LOP at an injection current of 350 mA. This is likely attributed to the low-stress and improved quality of epilayer grown on Gr/sapphire substrate. The inset of Figure 5b shows a photograph of as-fabricated LEDs on Gr/sapphire substrate with high brightness under injection current of 350 mA. The normalized EL spectra of as-fabricated LEDs with and without Gr interlayer under different injection current are shown in Figure 5c,d to evaluate the reliability. The LEDs with Gr only shows a faint variation due to the inevitable band filling effect and a screening effect by the internal polarization electric field, which is consistent with the low-stress property of GaN films obtained on Gr/sapphire substrates.[42] For comparison, the LED without Gr interlayer shows significant peak position blueshifts from 491.3 to 470.8 nm with increasing current to 700 mA and then redshifts to 480.4 nm under injection current of 800 mA owing to the high biaxial stress in epilayers probably due to the high TD density induced high indium contents in MQWs. Those results demonstrate that high-brightness and high-power LEDs can be fabricated on the sapphire substrate.

In summary, we successfully demonstrate the growth of low-stress and low dislocation density single-crystalline GaN film on Gr buffered sapphire substrates without other LT buffer layer and its application in high brightness, high-power blue LEDs. Scalable Gr/sapphire substrates are obtained by the direct grown APCVD method to avoid the tedious transfer process. N_2 plasma treatment creates sufficient nucleation centers for nitrides growth. The Gr buffer layer effectively releases the biaxial stress between GaN films and sapphire substrate, leading to the reduction of the dislocation density. The as-fabricated high-power LEDs on Gr/sapphire substrates show excellent electrical and optical properties superior to that of its conventional counterpart. Such one step of high-temperature MOCVD growth process compared to the conventional two-step method (initialed with low temperature and followed by high temperature) can shorten the MOCVD growth time and thus reduce the cost. Furthermore, since this method seems compatible with industrial manufacturing processes, we believe that incorporation of Gr into GaN-based devices is workable and can significantly enhance brightness of LEDs in future.

Experimental Section

CVD Growth of Gr on Sapphire Substrate: Typically, the commercial 2 in. *c*-sapphire substrate was cleaned with deionized water, ethanol, and acetone and then loaded into a three-zone high-temperature furnace. The furnace was heated to 1050 °C and stabilized about 10 min under 500 sccm Ar and 300 sccm H_2. 30 sccm CH_4 was introduced into the reaction chamber as carbon source for the growth of graphene on the sapphire substrate for about 3–5 h.

MOCVD Growth of GaN on Gr/Sapphire Substrate: The Gr/sapphire substrate was exposed to N_2 plasma treatment for 30 S with power of 100 W before being loaded into the MOCVD charmer. A much broader and up-shifted G band was observed in the Raman spectra with respect to pristine graphene. The G band peak position was shifted from 1592.6 to 1604.2 cm^{-1}, while the FWHM of G band was increased from 53.4 to 96.1 cm^{-1}. Trimethylgallium (TMGa), trimethylaluminum (TMAl), and NH_3 were used as Ga, Al, and N precursors for growing GaN and AlN films; triethylgallium and trimethylindium were used as Ga, In precursors for growing $In_xGa_{1-x}N$/GaN layers in the MQWs. First, the HT-AlN was grown at a nominal temperature of 1200 °C for 1 h with the NH_3 flow of 500 sccm and TMAl flow of 50 sccm (with AlN thickness being about 1.5 µm), respectively. It is a one-step process without using LT-buffer layer. Then u-GaN layer was grown at 1045 °C for 55 min with the NH_3 flow of 6000 sccm and TMGa flow of 80 sccm (with GaN thickness being about 2.0 µm), respectively, followed by a *n*-doped GaN layer with the silicane flow of 2.34 sccm. Then 11 periods of $In_xGa_{1-x}N$/GaN active layers were grown at 735 °C/834 °C with 3 nm InGaN well layers and 12 nm GaN barriers. The active layers were capped with a p-GaN layer deposited at 950 °C with the bis-cyclopentadienyl magnesium (Cp_2Mg) flow of 120 sccm, followed by an annealing process at 720 °C for 10 min under N_2 ambient.

LED Device Fabrication: LED devices with 45 mil^2 size were fabricated using a conventional mesa structure. First, ITO was deposited on top of p-GaN as a current-spreading layer. Then, photolithography and

© 2018 WILEY-VCH Verlag GmbH & Co. KGaA, Weinheim

15214095, 2018, 30, Downloaded from https://onlinelibrary.wiley.com/doi/10.1002/adma.201801608 by Peking University Health, Wiley Online Library on [03/09/2023]. See the Terms and Conditions (https://onlinelibrary.wiley.com/terms-and-conditions) on Wiley Online Library for rules of use; OA articles are governed by the applicable Creative Commons License

inductively coupled plasma etching were introduced to expose the n-GaN layer. Cr/Al/Ti/Au metals were deposited by electron beam evaporation as p/n contact electrodes, followed by a SiO_2 protection layer using plasma enhanced chemical vapor deposition method. Finally, the whole wafer was cut into pieces of devices and then packaged.

Characterization: The samples were characterized with optical microscopy (Olympus DX51), SEM (Hitachi S-4800; operating at 1 kV), Raman spectroscopy (Horiba, LabRAM HR-800; 514 nm laser excitation), ESEM (FEI Quanta 200F), AFM (Bruker Dimension Icon), XPS (Kratos Analytical Axis-Ultra spectrometer using a monochromatic Al Kα X-ray source), TEM (FEI Tecnai F20, operating at 200 kV), and aberration-corrected TEM (FEI Titan Cubed Themis G2 300) operated at 300 kV.

Supporting Information

Supporting Information is available from the Wiley Online Library or from the author.

Acknowledgements

Z.L.C., X.Z., and Z.P.D. contributed equally to this work. This work was financially supported by the National Basic Research Program of China (Grant No. 2016YFA0200103), the National Key R&D Program of China (Grant Nos. 2018YFB0406703, 2016YFB0400102, and 2016YFB04000803), the National Natural Science Foundation of China (Grant Nos. 51432002, 61474109, 51290272, 51502007, 11474247, and 51672007), the National Equipment Program of China (Grant No. ZDYZ2015-1), the Beijing Municipal Science and Technology Planning Project (Grant Nos. Z161100002116020 and Z161100002116032), and the Beijing Natural Science Foundation (Grant No. 4182063). The authors thank Dr. Xujing Li, Mingqiang Li, and Ning Li for their help in TEM analysis. P.G. acknowledges support from the National Program for Thousand Young Talents of China and "2011 Program" Peking-Tsinghua-IOP Collaborative Innovation Center of Quantum Matter. The authors also acknowledge Electron Microscopy Laboratory in Peking University for the use of Cs corrected electron microscope.

Conflict of Interest

The authors declare no conflict of interest.

Keywords

chemical vapor deposition, gallium nitride, graphene, light-emitting diodes

Received: March 12, 2018
Revised: April 18, 2018
Published online: June 8, 2018

[1] C. Lee, X. Wei, J. W. Kysar, J. Hone, *Science* **2008**, *321*, 385.
[2] K. S. Novoselov, A. K. Geim, S. V. Morozov, D. Jiang, Y. Zhang, S. V. Dubonos, I. V. Grigorieva, A. A. Firsov, *Science* **2004**, *306*, 666.
[3] A. A. Balandin, *Nat. Mater.* **2011**, *10*, 569.
[4] R. R. Nair, P. Blake, A. N. Grigorenko, K. S. Novoselov, T. J. Booth, T. Stauber, N. M. R. Peres, A. K. Geim, *Science* **2008**, *320*, 1308.
[5] I. Meric, M. Y. Han, A. F. Young, B. Ozyilmaz, P. Kim, K. L. Shepard, *Nat. Nanotechnol.* **2008**, *3*, 654.
[6] R. Raccichini, A. Varzi, S. Passerini, B. Scrosati, *Nat. Mater.* **2015**, *14*, 271.
[7] S.-W. Liu, H.-P. Wang, Q. Xu, T.-B. Ma, G. Yu, C. Zhang, D. Geng, Z. Yu, S. Zhang, W. Wang, Y.-Z. Hu, H. Wang, J. Luo, *Nat. Commun.* **2017**, *8*, 14029.
[8] T.-H. Han, Y. Lee, M.-R. Choi, S.-H. Woo, S.-H. Bae, B. H. Hong, J.-H. Ahn, T.-W. Lee, *Nat. Photonics* **2012**, *6*, 105.
[9] T.-H. Han, H. Kim, S.-J. Kwon, T.-W. Lee, *Mater. Sci. Eng. R Rep.* **2017**, *118*, 1.
[10] T.-H. Han, M.-H. Park, S.-J. Kwon, S.-H. Bae, H.-K. Seo, H. Cho, J.-H. Ahn, T.-W. Lee, *NPG Asia Mater.* **2016**, *8*, e303.
[11] J. Kim, C. Bayram, H. Park, C.-W. Cheng, C. Dimitrakopoulos, J. A. Ott, K. B. Reuter, S. W. Bedell, D. K. Sadana, *Nat. Commun.* **2014**, *5*, 4836.
[12] K. Chung, C.-H. Lee, G.-C. Yi, *Science* **2010**, *330*, 655.
[13] F. Xia, T. Mueller, Y.-M. Lin, A. Valdes-Garcia, P. Avouris, *Nanotechnology* **2009**, *4*, 839.
[14] T. R. Nayak, H. Andersen, V. S. Makam, C. Khaw, S. Bae, X. Xu, P.-L. R. Ee, J.-H. Ahn, B. H. Hong, G. Pastorin, B. Oezyilmaz, *ACS Nano* **2011**, *5*, 4670.
[15] S. Nakamura, M. R. Krames, *Proc. IEEE* **2013**, *101*, 2211.
[16] J. K. Sheu, S. J. Chang, C. H. Kuo, Y. K. Su, L. W. Wu, Y. C. Lin, W. C. Lai, J. M. Tsai, G. C. Chi, R. K. Wu, *IEEE Photonics Technol. Lett.* **2003**, *15*, 18.
[17] S. Fernandez-Garrido, M. Ramsteiner, G. Gao, L. A. Galves, B. Sharma, P. Corfdir, G. Calabrese, Z. d. S. Schiaber, C. Pfueller, A. Trampert, J. M. J. Lopes, O. Brandt, L. Geelhaar, *Nano Lett.* **2017**, *17*, 5213.
[18] L. Wang, W. Liu, Y. Zhang, Z.-H. Zhang, S. T. Tan, X. Yi, G. Wang, X. Sun, H. Zhu, H. V. Demir, *Nano Energy* **2015**, *12*, 419.
[19] Z. Li, J. Kang, Y. Zhang, Z. Liu, L. Wang, X. Lee, X. Li, X. Yi, H. Zhu, G. Wang, *J. Appl. Phys.* **2013**, *113*, 234302.
[20] T. H. Seo, T. S. Oh, S. J. Chae, A. H. Park, K. J. Lee, Y. H. Lee, E.-K. Suh, *Jpn. J. Appl. Phys.* **2011**, *50*, 125103.
[21] H. Nam, C. Tran Viet, M. Han, B. D. Ryu, S. Chandramohan, J. B. Park, J. H. Kang, Y.-J. Park, K. B. Ko, H. Y. Kim, H. K. Kim, J. H. Ryu, Y. S. Katharria, C.-J. Choi, C.-H. Hong, *Nat. Commun.* **2013**, *4*, 1452.
[22] C.-H. Lee, Y.-J. Kim, Y. J. Hong, S.-R. Jeon, S. Bae, B. H. Hong, G.-C. Yi, *Adv. Mater.* **2011**, *23*, 4614.
[23] L. Zhang, X. L. Li, Y. L. Shao, J. X. Yu, Y. Z. Wu, X. P. Hao, Z. M. Yin, Y. B. Dai, Y. Tian, Q. Huo, Y. N. Shen, Z. Hua, B. G. Zhang, *ACS Appl. Mater. Interfaces* **2015**, *7*, 4504.
[24] A. H. Park, T. H. Seo, S. Chandramohan, G. H. Lee, K. H. Min, S. Lee, M. J. Kim, Y. G. Hwang, E.-K. Suh, *Nanoscale* **2015**, *7*, 15099.
[25] J. H. Son, J.-L. Lee, *Opt. Express* **2010**, *18*, 5466.
[26] U. V. Patil, A. S. Pawbake, L. G. B. Machuno, R. V. Gelamo, S. R. Jadkar, C. S. Rout, D. J. Late, *RSC Adv.* **2016**, *6*, 48843.
[27] R. T. Khare, R. V. Gelamo, M. A. More, D. J. Late, C. S. Rout, *Appl. Phys. Lett.* **2015**, *107*, 123503.
[28] A. S. Pawbake, K. K. Mishra, L. G. B. Machuno, R. V. Gelamo, T. R. Ravindran, C. S. Rout, D. J. Late, *Diamond Relat. Mater.* **2018**, *84*, 146.
[29] D. J. Late, *Adv. Device Mater.* **2015**, *1*, 52.
[30] Y. Alaskar, S. Arafin, D. Wickramaratne, M. A. Zurbuchen, L. He, J. McKay, Q. Lin, M. S. Goorsky, R. K. Lake, K. L. Wang, *Adv. Funct. Mater.* **2014**, *24*, 6629.
[31] Y. Kim, S. S. Cruz, K. Lee, B. O. Alawode, C. Choi, Y. Song, J. M. Johnson, C. Heidelberger, W. Kong, S. Choi, K. Qiao, I. Almansouri, E. A. Fitzgerald, J. Kong, A. M. Kolpak, J. Hwang, J. Kim, *Nature* **2017**, *544*, 340.
[32] Y. Yao, Y. Ishikawa, M. Sudo, Y. Sugawara, D. Yokoe, *J. Cryst. Growth* **2017**, *468*, 484.

© 2018 WILEY-VCH Verlag GmbH & Co. KGaA, Weinheim

15214095, 2018, 30, Downloaded from https://onlinelibrary.wiley.com/doi/10.1002/adma.201801608 by Peking University Health, Wiley Online Library on [03/09/2023]. See the Terms and Conditions (https://onlinelibrary.wiley.com/terms-and-conditions) on Wiley Online Library for rules of use; OA articles are governed by the applicable Creative Commons License

[33] G. S. Wang, H. Lu, D. J. Chen, F. F. Ren, R. Zhang, Y. D. Zheng, *IEEE Photonics Technol. Lett.* **2013**, *25*, 652.
[34] H. Lu, X. A. Cao, S. F. LeBoeuf, H. C. Hong, E. B. Kaminsky, S. D. Arthur, *J. Cryst. Growth* **2006**, *291*, 82.
[35] J. H. Ryu, Y. S. Katharria, H. Y. Kim, H. K. Kim, K. B. Ko, N. Han, J. H. Kang, Y. J. Park, E. K. Suh, C. H. Hong, *Appl. Phys. Lett.* **2012**, *100*, 181904.
[36] T. B. Wei, R. F. Duan, J. X. Wang, J. M. Li, Z. Q. Huo, P. Ma, Z. Liu, Y. P. Zeng, *J. Phys. D: Appl. Phys.* **2007**, *40*, 2881.
[37] H. Heinke, V. Kirchner, S. Einfeldt, D. Hommel, *Appl. Phys. Lett.* **2000**, *77*, 2145.
[38] V. Srikant, J. S. Speck, D. R. Clarke, *J. Appl. Phys.* **1997**, *82*, 4286.
[39] H. Lahreche, P. Vennegues, O. Tottereau, M. Laugt, P. Lorenzini, M. Leroux, B. Beaumont, P. Gibart, *J. Cryst. Growth* **2000**, *217*, 13.
[40] Y.-H. Ra, R. Navamathavan, J.-H. Park, C.-R. Lee, *ACS Appl. Mater. Interfaces* **2013**, *5*, 2111.
[41] J. Goldberger, R. R. He, Y. F. Zhang, S. W. Lee, H. Q. Yan, H. J. Choi, P. D. Yang, *Nature* **2003**, *422*, 599.
[42] E. Kuokstis, J. W. Yang, G. Simin, M. A. Khan, R. Gaska, M. S. Shur, *Appl. Phys. Lett.* **2002**, *80*, 977.

© 2018 WILEY-VCH Verlag GmbH & Co. KGaA, Weinheim

15214095, 2018, 30, Downloaded from https://onlinelibrary.wiley.com/doi/10.1002/adma.201801608 by Peking University Health, Wiley Online Library on [03/09/2023]. See the Terms and Conditions (https://onlinelibrary.wiley.com/terms-and-conditions) on Wiley Online Library for rules of use; OA articles are governed by the applicable Creative Commons License